



A Comparative Study of Six Hybrid Prediction Models for Uniaxial Compressive Strength of Rock Based on Swarm Intelligence Optimization Algorithms

Yu Lei, Shengtao Zhou, Xuedong Luo*, Shuaishuai Niu and Nan Jiang

Faculty of Engineering, China University of Geosciences, Wuhan, China

OPEN ACCESS

Edited by:

Guang-Liang Feng,
Institute of Rock and Soil Mechanics
(CAS), China

Reviewed by:

Quan Jiang,
Institute of Rock and Soil Mechanics
(CAS), China

Renguo Gu,
South China University of Technology,
China

Yi Luo,
Wuhan University of Technology,
China

*Correspondence:

Xuedong Luo
cugluoxd@foxmail.com

Specialty section:

This article was submitted to
Geohazards and Georisks,
a section of the journal
Frontiers in Earth Science

Received: 27 April 2022

Accepted: 23 May 2022

Published: 01 July 2022

Citation:

Lei Y, Zhou S, Luo X, Niu S and Jiang N
(2022) A Comparative Study of Six
Hybrid Prediction Models for Uniaxial
Compressive Strength of Rock Based
on Swarm Intelligence
Optimization Algorithms.
Front. Earth Sci. 10:930130.
doi: 10.3389/feart.2022.930130

Uniaxial compressive strength (UCS) is a significant parameter in mining engineering and rock engineering. The laboratory rock test is time-consuming and economically costly. Therefore, developing a reliable and accurate UCS prediction model through easily obtained rock parameters is a good way. In this paper, we set five input parameters and compare six hybrid models based on BP neural network and six swarm intelligence optimization algorithms—bird swarm algorithm (BSA), grey wolf optimization (GWO), whale optimization algorithm (WOA), seagull optimization algorithm (SOA), lion swarm optimization (LSO), firefly algorithm (FA) with the accuracy of two single models without optimization—BP neural network and random forest algorithm. Finally, the above eight models were evaluated and compared by root mean square error (RMSE), mean absolute percentage error (MAPE), coefficient of determination (R^2), and a10 index to obtain the most suitable prediction model. It is indicated that the best prediction model is the FA-BP model, with a RMSE value of 4.883, a MAPE value of 0.063, and a R^2 of 0.985, and an a10 index of 0.967. Furthermore, the normalized mutual information sensitivity analysis shows that point load strength is the most effective parameters on the UCS, respectively.

Keywords: uniaxial compressive strength, rock, BP neural network, swarm intelligence optimization algorithm, normalized mutual information

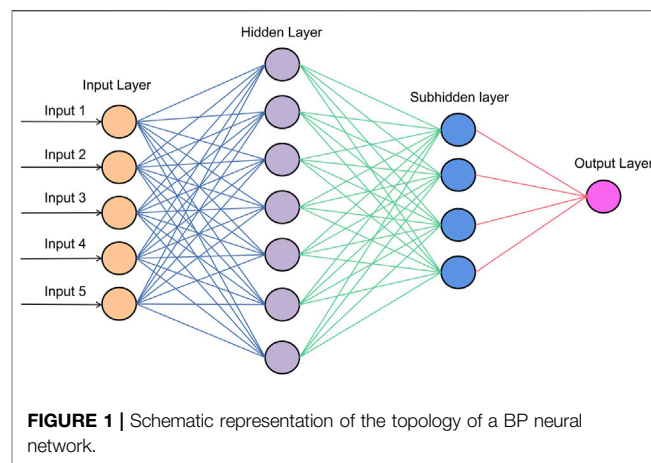
INTRODUCTION

Uniaxial compressive strength is an important metric in rock mechanics and rock engineering, particularly in the evaluation of rock slope stability, tunneling design, and ore mining. On the other hand, the laboratory UCS test is time-consuming and costly. Many predict approaches have been offered to acquire the UCS quickly and cheaply.

The association between the physical and mechanical properties of rock samples and the UCS should be studied before the UCS can be predicted. Previous studies have found that a lot of rock parameters such as porosity, longitudinal wave velocity, point load strength, density, block impulse index (BPI), Young's modulus, Schmidt hammer rebound number were correlated with UCS (Bieniawski, 1978; Barton et al., 1980; Nicholson and Bieniawski, 1990; Mitri et al., 1994; Hoke and Brown, 1997; Barton, 2002; Tsiambaos and Sabatakakis, 2004; Hao et al., 2018; Shan and Lai, 2018; He et al., 2019). After determining the parameters that are closely related to UCS, scholars usually use the empirical equation prediction method and machine learning methods to predict the UCS by these parameters.

When using the empirical equation to predict the UCS, scholars selected one or more parameters of rock samples and fit the statistical relationship between them and UCS. Part of scholars choose a single parameter and make predictions through different types of empirical equations. Leite and Ferland (2001) took the porosity as the input variable, carried out the linear fitting between the porosity and UCS, and found that the porosity and UCS were negatively correlated. Lashkaripour (2002) investigated the relationship between the porosity and the UCS by the exponential function, a similar conclusion was obtained with Leite and Ferland. Yasar and Erdogan (2004) conducted linear fitting on the longitudinal wave velocity and UCS. Yilmaz and Sendir (2002) fitted the Schmidt hammer rebound number and UCS with a function combining logarithmic function and linear function and obtained a reliable UCS prediction equation. Broch and Franklin (1972) corrected the size of rock samples to obtain the point load strength, established a linear function between the point load strength and UCS, and found that these two parameters are closely related. Ulusay and Gokceglu (1998) developed a block impulse index test device, using the BPI as a parameter to indirectly evaluate UCS, and fitting it with a power function. Yagiz (2011) found that the slake durability index could be selected as an input variable for predicting UCS. Moreover, some scholars choose a variety of rock parameters to conduct this work. Sachpazis (1990) tested the UCS, Young's modulus, and Schmidt hammer rebound number and established a regression equation between the three. Kayabasi et al. (2003) thought UCS was related to RQD value, Young's modulus, and weathering degree of rock samples, and fit these three parameters and UCS, and the established a regression equation could meet the requirement. On the whole, the fitting equation proposed with the traditional statistical methods could meet the needs of projects.

With the development of advanced artificial intelligence methods, various non-linear UCS prediction models have been established. In these models, several physical and mechanical parameters of rock samples are usually chosen at the same time as the input variables. Through tensile strength, point load strength, and Young's modulus, Armaghani et al. (2015) used the multiple regression analysis (MRA) and an adaptive neuro-fuzzy inference system (ANFIS) to obtain the UCS. Meulenkamp and Grima (1999) used Young's modulus, porosity, and density to predict UCS by the artificial neural network, and accurate prediction results were obtained. By using longitudinal BPI, Schmidt hammer rebound number, and wave velocity, point load index, Mishra and Basu et al. (2013) predicted the UCS with the farthest candidate selection model. The results indicated that Schmidt hammer rebound number and point load strength are excellent input variables. However, in the UCS prediction of shale, the longitudinal wave velocity is not a suitable input parameter. Rezaei et al. (2012) selected three parameters of density, Schmidt hammer rebound number, and porosity as the input variables, then the UCS was predicted by the fuzzy inference system (FIS). As a result, the predicted values were quite close to the laboratory-measured values. Furthermore, in this study, the sensitivity analysis showed that the Schmidt hammer rebound number was the best input variable among them. Mahmoodzadeh et al. (2021) chose long short term memory, deep neural networks, K-nearest neighbor, decision tree, and support vector regression to predict the UCS, and these models



all got good prediction results. Even if these single prediction models could effectively predict the UCS, combined optimization algorithms are gradually being applied. Majdi and Beiki (2010) established a genetic algorithm-optimized artificial neural network model to predict the UCS with density, RQD value, and porosity. The predicted results showed that better results could be obtained by the optimized model. Although the selected input variables are different, Mohamad et al. (2015) and Momeni et al. (2015) both employed the artificial neural network (ANN) combined with the particle swarm optimization (PSO) for the UCS prediction, the predicted results show that the optimized artificial neural network could give better-predicted values than before. On the basis of BPI, point load strength, Schmidt hammer rebound number, and longitudinal wave velocity, Xue and Wei (2020) compare the predicted results of least-squares support vector machine (LSSVM) optimized by genetic algorithm, ANFIS, FIS, and ANN. The optimized models' accuracy is superior to the other three single models, according to the anticipated outcomes. Compared with the empirical equation prediction method, the prediction models established through different artificial intelligence algorithms have better performance in UCS prediction.

Although models built by artificial intelligence algorithms have found many applications in predicting UCS, its hybrid model building and the selection of input parameters still need to be refined. To find a suitable prediction algorithm and input parameters to predict UCS, in this paper, we selected five input parameters and used the six optimized BP neural networks with different swarm intelligence algorithms to predict the UCS, and evaluated the models through multiple evaluation indexes to find the optimal UCS prediction model. The findings of the study may be used as a reference to determine UCS quickly.

BASIC CONCEPTS AND ALGORITHMS OF PREDICT MODELS

BP Neural Network

The input layer, middle layers, and output layer make up a BP neural network, with all neurons in the input and middle layers and the output layer linked. It is worth noting that neurons in the

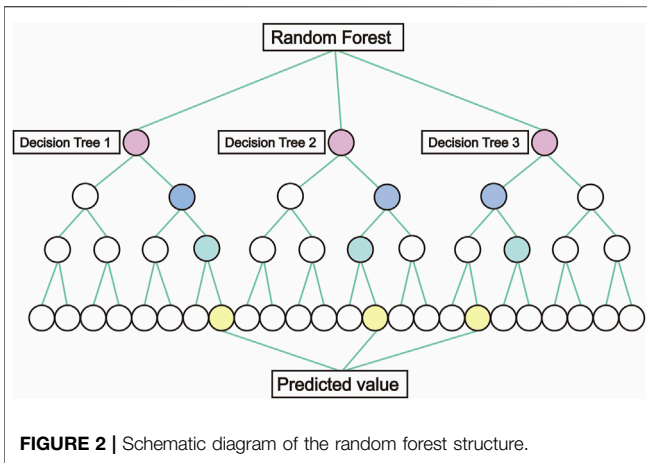


FIGURE 2 | Schematic diagram of the random forest structure.

relationship between input and output data, which leads to this method being used in multivariate non-linear system analysis.

Random Forest Algorithm

Leo Breiman (2001) invented the Random Forest (RF) method, which is a classic machine learning approach, which integrates multiple decision trees through integration learning (Bureau et al., 2010). Decision tree is a tree-like structure **Figure 2** in which any internal node represents an attribute test. Each branch in decision tree represents an output result, and each leaf node represents a type. Within the integrated learning, multiple classifiers are generated, each classifier conducts learning and prediction without interfering and finally synthesizing a single prediction. The most widely used algorithms in integrated learning are the bagging algorithm and the boosting algorithm.

More explanations regarding the FA algorithm can be found in the literature (Yu et al., 2020a; Yu et al., 2020b; Yin et al., 2022).

same layer are not linked. (Yan and Zeng, 2013). The topology of a BP neural network is shown in **Figure 1**. Through learning the input data, BP neural networks could establish a mapping

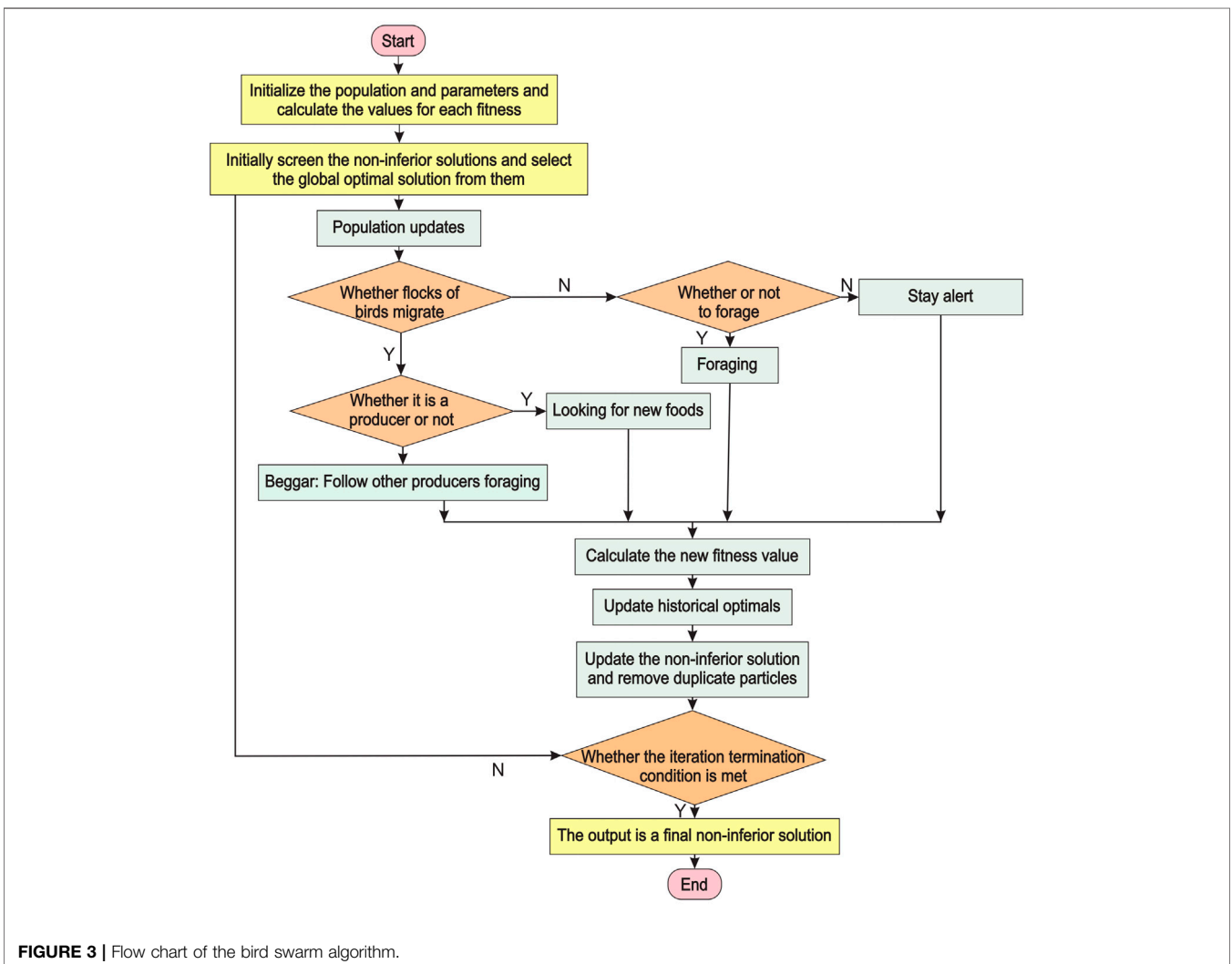


FIGURE 3 | Flow chart of the bird swarm algorithm.

Bird Swarm Algorithm

Bird is one of the flocking animals, and there are behaviors such as foraging, vigilance, and flight in their life (Meng et al., 2014). Bird swarm algorithm (BSA) is proposed inspired by these behaviors of birds. These community behaviors may be mimicked, and the swarm’s state of foraging, vigilance, and flight could be changed using precise rules. The analogous equation while the swarm is foraging is as follows:

$$x_{i,j}^{t+1} = x_{i,j}^t + rand(0, 1) \times C \times (p_{i,j} - x_{i,j}^t) + rand(0, 1) \times S \times (g_j - x_{i,j}^t) \tag{1}$$

Where j is a positive integer between 1 and D , $rand(0,1)$ is a uniformly distributed random number between 0 and 1, C is the cognitive acceleration factor, S is the social acceleration factor, and both C and S are positive integers, $p_{i,j}$ is the previous optimal position of the i th bird, and g_j represents the previous optimal position in the swarm.

When the swarm is alert, each bird tries to get closer to the swarm’s center. However, there is competition between every bird so that each bird does not move directly towards the swarm center. The flow chart of the BSA is shown in **Figure 3**. More explanations regarding the BSA algorithm can be found in the literature (Meng et al., 2015; Miramontes et al., 2018; Varol Altay and Alatas, 2019).

Grey Wolf Optimization

Grey wolf optimization (GWO) is a new meta-heuristic algorithm inspired by the grey wolf population’s social structure. (Mirjalili and Lewis, 2016). There are four different types of grey wolves, α , β , Δ , and ω , in the social hierarchy. The α wolf has the highest status, followed by the β wolf, then the Δ wolf, and the lowest rank is the ω wolf. Moreover, Hunting behavior is divided into three steps—locking for prey, surrounding the prey, and attacking the prey (Kishor and Singh, 2016).

In the beginning, the wolves approach the prey by stalking and chasing. Then a group of grey wolves will surround the prey until the prey stops moving. Finally, they attack the prey. The behaviors of a wolf population could be defined as:

$$\vec{D}_G = \left| \vec{C}_G \cdot \vec{X}_{PG}(t_G) - \vec{X}_G(t_G) \right| \tag{2}$$

$$\vec{X}_G(t + 1) = \vec{X}_{PG}(t) - \vec{A}_G \cdot \vec{D}_G \tag{3}$$

Where \vec{D}_G is the distance between the wolf and the prey, \vec{X}_{PG} is the prey position vector, \vec{X}_G is the position vector of the grey wolf, t_G is the number of current iterations, \vec{A}_G and \vec{D}_G are the coefficient vectors. For a complete detail of the GWO algorithm, the readers can refer to the study conducted by Yu et al. (2019) and Yu et al. (2020c).

Whale Optimization Algorithm

Whales tend to hunt little fish at the surface of the ocean. Their feeding journey is a unique spiral upward path with many distinctive bubbles (Mirjalili and Lewis, 2016). There are three common behaviors in whales, searching for prey, surrounding prey, and hunting in the whale optimization algorithm (WOA).

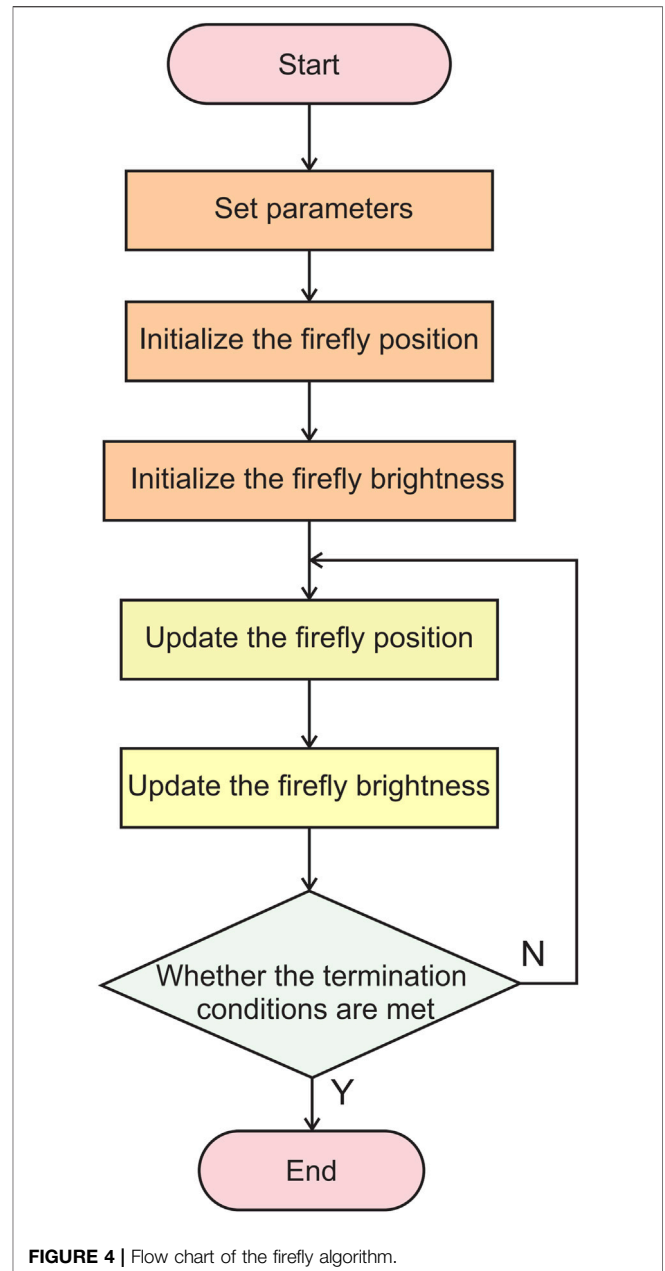


FIGURE 4 | Flow chart of the firefly algorithm.

Before hunting the prey, when \vec{A}_W is greater than 1 or less than -1 , the whale in the group randomly selects prey referring to each other’s positions so that the global search ability would be improved, this behavior could be written as:

$$\vec{D}_W = \left| \vec{C}_W \cdot \vec{X}_{rand}(t_W) - \vec{X}_W(t_W) \right| \tag{4}$$

$$\vec{X}_W(t_W + 1) = \vec{X}_{rand}(t_W) - \vec{A}_W \cdot \vec{D}_W \tag{5}$$

Where \vec{X}_{rand} is the randomly chosen location variable for the current whale population, \vec{D}_W is the distance between the whale and the prey; \vec{X}_W is the position vector of the optimal solution, t_W is the number of current iterations, \vec{A}_W and C_W are both the

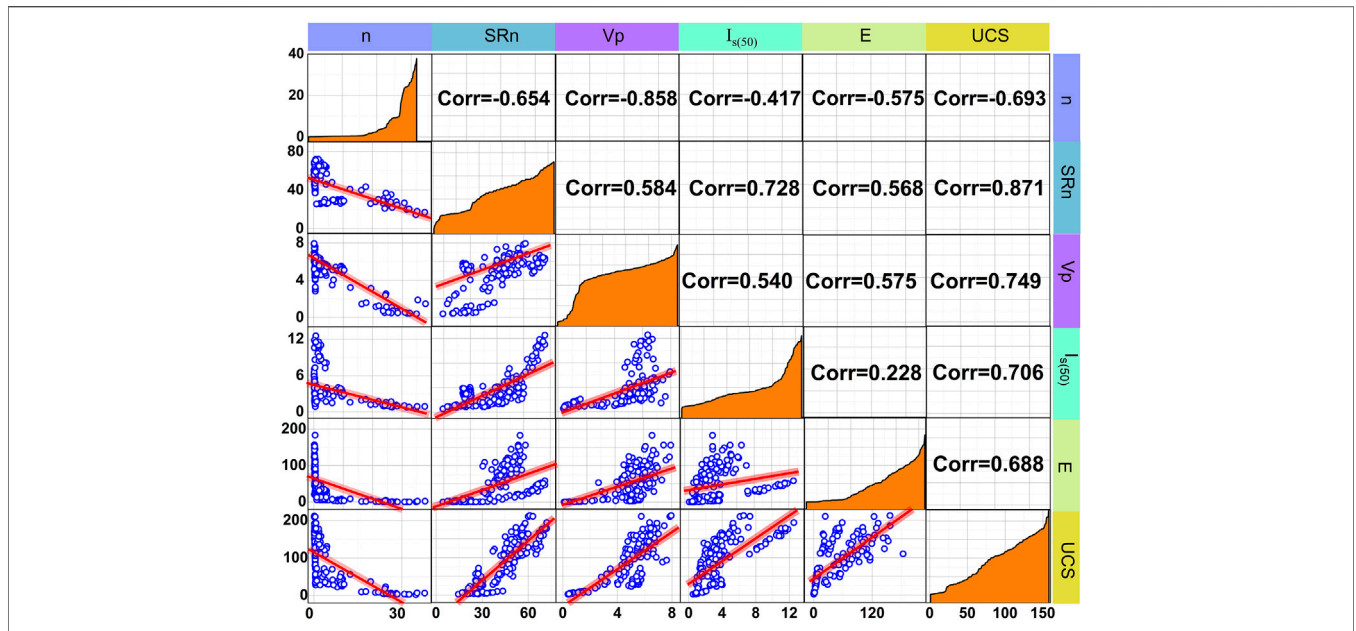


FIGURE 5 | Data matrix.

coefficient vectors. For more details, equations and implementation process of the WOA can be referred to the published studies in literature (Aljarah et al., 2016; Mirjalili and Lewis, 2016; Mafarja and Mirjalili, 2017).

Seagull Optimization Algorithm

Migrating and feeding are the most essential characteristics of seagulls, and the seagull optimization method is based on these activities. To avoid colliding, each bird is at a distinct place. Seagulls may fly towards the direction of the best landing spot. Seagull groups maneuver in a spiral manner when hunting for prey. (Dhiman and Kumar, 2019).

To avoid colliding with other seagulls as they migrate, the new position of the seagull might be determined using the additional variable *A* as follows:

$$C_s(t_s) = A \times P_s(t_s) \tag{6}$$

Where *C_s* is a new position that is not in conflict with other seagulls, *P_s* is the seagull's present location, *t_s* is the current iteration. *A* reflects the seagull's movement behavior in the given search space, and it may be calculated as:

$$A = f_c - [t_s \times (f_c / MAX_{iteration})] \tag{7}$$

Where *f_c* is the frequency of the control variable *A*, with a value linearly decreasing from 2 to 0. To have a better understanding regarding the SOA optimization technique, other studies in literature can be considered (Dhiman and Kumar, 2019; Dhiman et al., 2020; Panagant et al., 2020).

Lion Swarm Optimization

Lion swarm optimization is a new intelligence optimization algorithm proposed to simulate lion hunting. There are three

types of lions in the population: lion king, lioness, and young lion. The update of their position follows different rules. The algorithm initializes the lion pride positions. Similar to other swarm intelligence optimization algorithms, the parameters in LSO need to be initialized before optimization starts (Yazdani and Jolai, 2016).

The lion king travels in a small area around the best prey during hunting, and the corresponding position update equation is:

$$X_m^{t+1} = g^{tL} (1 + \gamma(p_m^{tL} - g^{tL})) \tag{8}$$

Where *X_m* is the update position of the lion king, *γ* is a random number that fits a normal distribution between *N*(0,1); *g^{tL}* is the population optimal solution in the *t_L*th iteration; and *p_m^{tL}* is the historical optimal solution for the *m*th individual in the *t_L*th iteration.

Through collaborative hunting, lionesses catch their prey, and this behavior can be described as:

$$X_i^{t+1} = \frac{P_i^{tL} + P_c^{tL}}{2} (1 + \alpha_f \gamma) \tag{9}$$

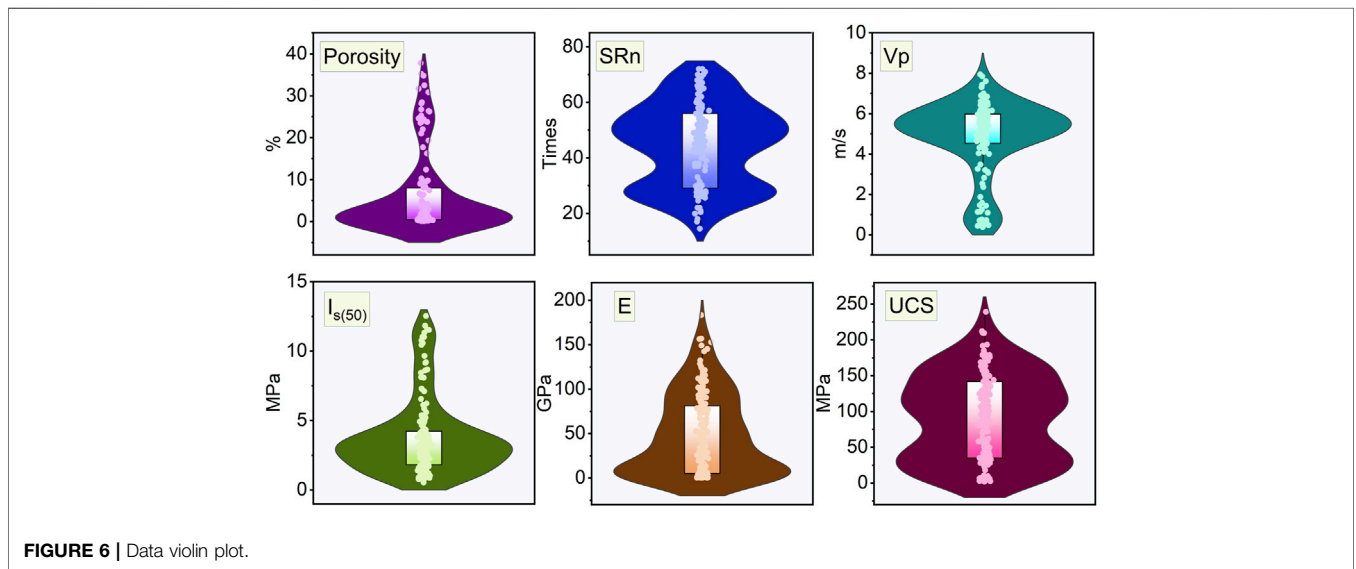
Where *X* is the position of the lioness moving, *P_c^{tL}* is the historical optimal solution for a randomly selected predation partner in the lioness' pride during the *t_L* iteration; *α_f* is the lioness' range perturbation factor, which mainly affects the lioness' range of movement so that the lioness can search for prey at a larger range and reduce the enclosure after finding prey. A complete version of the LSO optimization algorithm can be seen in previous work (Yazdani and Jolai, 2016).

Firefly Algorithm

Firefly algorithm (FA) is a group search-based stochastic optimization algorithm. There are a few parameters in FA. No

TABLE 1 | Rock sample data.

No.	Type	Location	Porosity (%)	SRn	V _p (km/s)	I _s (50)(MP)	E (GPa)	UCS (MPa)
1	Granite	Malaysia	0.39	47	5.506	2.31	92.9	117.9
2	Granite	Malaysia	0.44	38	6.45	2.87	108.8	122.3
3	Granite	Malaysia	0.25	45	5.95	3.12	78.4	124.7
4	Travertine	Haji	3.35	27.42	5.66	3.00	11.45	63.68
5	Travertine	Haji	9.35	27.38	5.38	2.86	8.03	47.46
6	Travertine	Haji	8.14	30.13	5.09	3.63	6.15	37.89
7	Caliche	Adana area	28.12	28.00	0.68	1.13	0.55	5.63
8	Caliche	Adana area	28.44	25.00	0.49	0.97	0.19	3.37
9	Caliche	Adana area	21.00	28.00	1.15	1.25	0.88	7.85
.....
153	Sandstone	Southern Anatolia	2.32	52.00	4.75	3.30	18.10	122.00
154	Limestone	Southern Anatolia	0.66	59.00	5.84	2.20	15.90	112.00
155	Granite	Çatalca	0.20	67.00	6.37	10.58	45.09	165.79
156	Granite	Kapıdağ	0.71	72.00	6.36	12.53	58.50	193.33
157	Granite	Kapıdağ	0.21	69.00	6.69	11.83	51.20	175.49
158	Tonalite	Gönen	1.70	68.00	5.84	10.77	48.61	157.62



complex operations such as variation and crossover, and the corresponding flow chart is shown in **Figure 4**.

There are two pivotal parameters in this method—light intensity and attractiveness (Gandomi et al., 2011).

The light intensity function can be described as:

$$I(r_{ij}) = I_0 e^{-\gamma r_{ij}^2} \tag{10}$$

Where I_0 is the initial light intensity of the firefly, r is the distance between two fireflies, γ is defined as the light intensity absorption coefficient, which could describe light lost in the propagation.

If two fireflies i and j are located at \vec{X}_{iF} and \vec{X}_{jF} , respectively, the distance between them can be calculated through Euclidean distance as:

$$r_{ij} = \|\vec{X}_{iF} - \vec{X}_{jF}\| = \sqrt{\sum_{k=1}^D (X_{ik} - X_{jk})^2} \tag{11}$$

Where D is the spatial dimension of the solution problem, X_{ik} is the coordinates of the i_{th} firefly in the k_{th} dimension.

The attractiveness of FA diminishes monotonically as the distance between them increases, and the attractiveness function $\beta(r)$ could be defined as.

$$\beta(r) = \beta_0 e^{-\gamma r^2} \tag{12}$$

Where β_0 is the attraction at the light source. A complete version of the FA optimization algorithm can be seen in previous works (Fister et al., 2013; Gandomi et al., 2013).

TABLE 2 | Initial parameters for hybrid model optimization.

Algorithm	Parameters	Value	Optimal parameters
BSA	a1	1	num_boosting_rounds = 2517 eta=0.0394
	a2	1	
	c	1	
	S	1	
	FQ	5	
	N	20	
GWO	Convergence constant a	[2,0]	num_boosting_rounds = 2612 eta=0.0262
WOA	r	[0,1]	num_boosting_rounds = 2371 eta=0.031
	a	[0,2]	
	b	1	
	l	[0,1]	
SOA	f _c	2	num_boosting_rounds = 795 eta=0.031
	r _d	[0,1]	
LSO	γ	0.5	num_boosting_rounds = 2290 eta=0.035
	α _t	0.4	
	α _c	0.4	
FA	γ	1	num_boosting_rounds = 262 eta=0.021
	β ₀	2	
	α	0.2	
	rand	0.98	

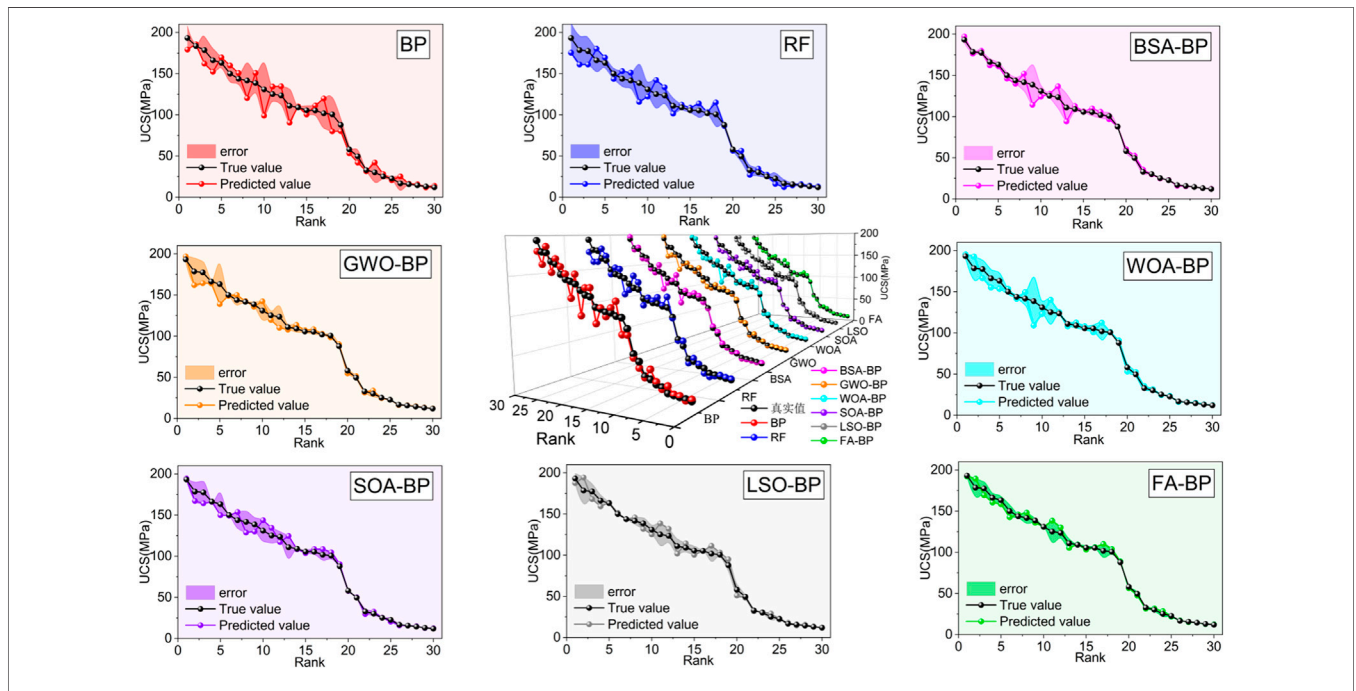


FIGURE 7 | Predicted vs. true values.

DATABASE AND DATA PRESENTATION

Selection of Input and Output Parameters

There are five input parameters—porosity, Schmidt hammer rebound number, longitudinal wave velocity, point load

strength, Young’s modulus, and one output parameter—the UCS in this paper. The first four input parameters could be obtained through non-destructive testing methods (Stroffek and Lesso, 2001; Liu et al., 2020). Moreover, the point load strength is easy to obtain in the field test. These five

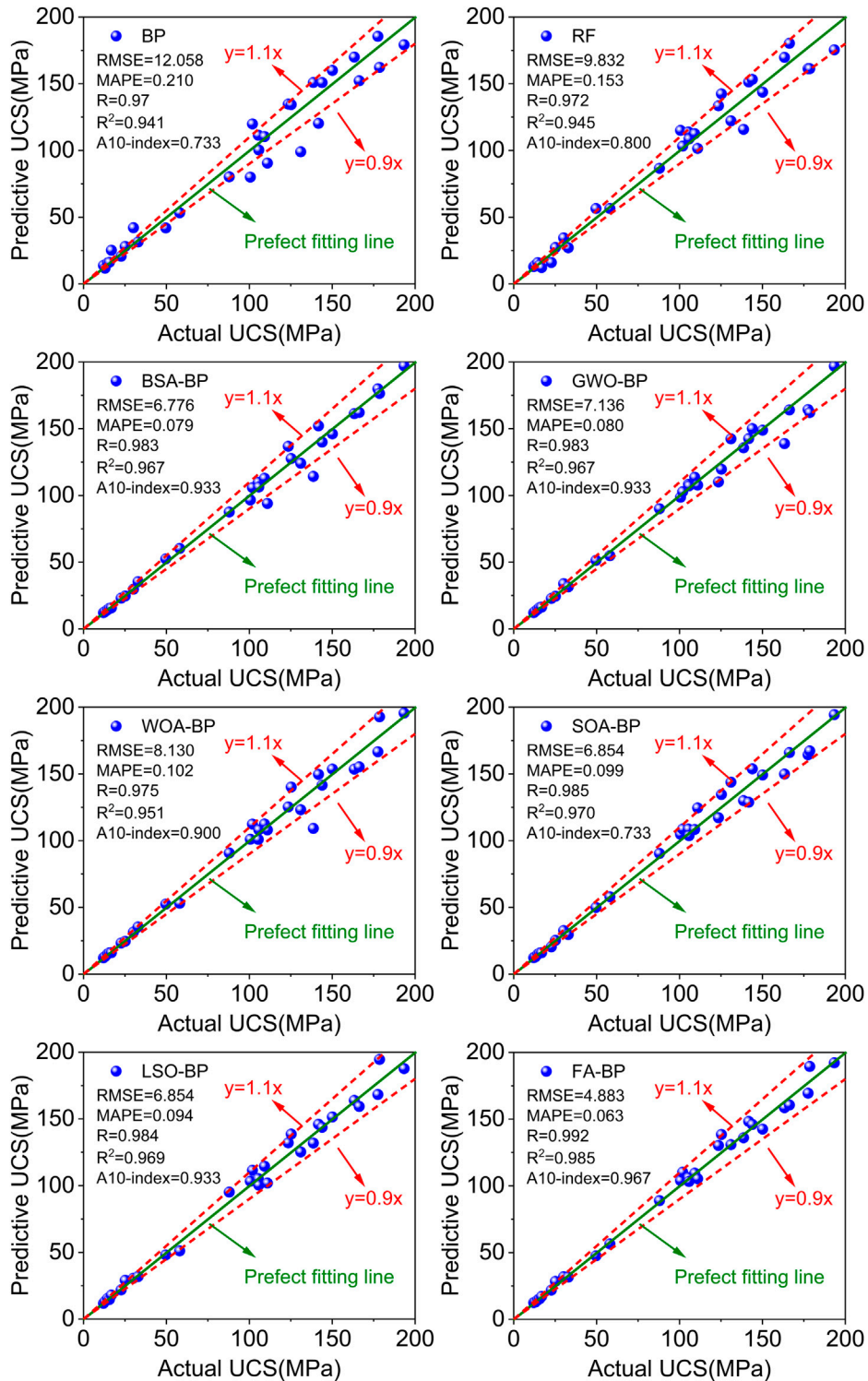


FIGURE 8 | Correlation analysis between predicted and actual values.

parameters have been used more often in many previous similar prediction models and are trustworthy parameters.

Database

The experimental data from the literature (Tugrul and Zarif, 1999; Dincer et al., 2008; Dehghan et al., 2010; Armaghani

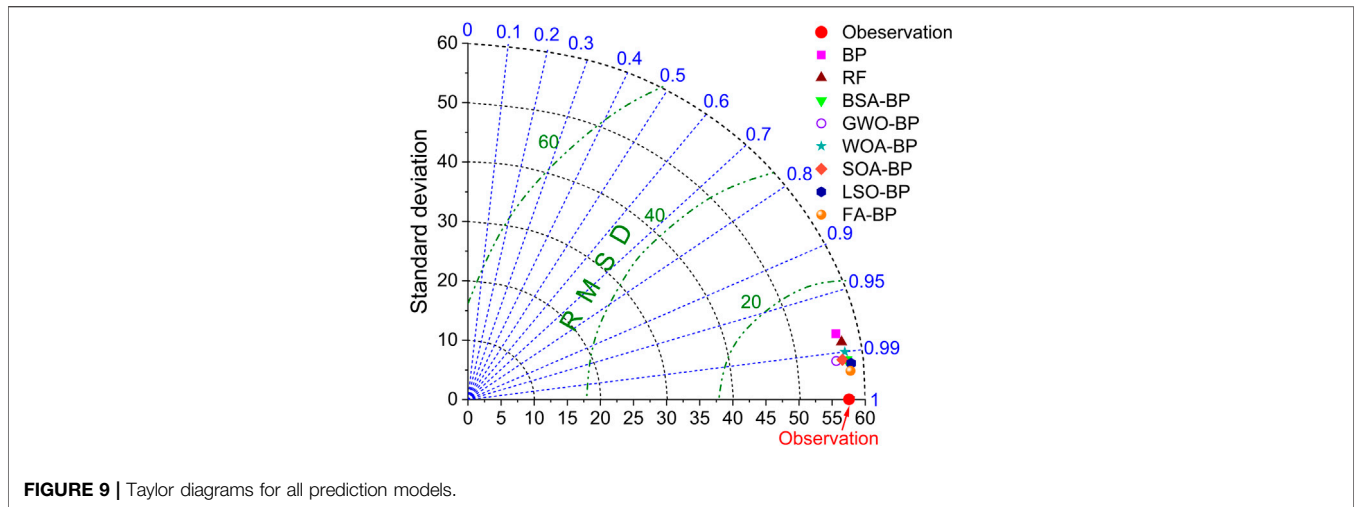


FIGURE 9 | Taylor diagrams for all prediction models.

et al., 2015) were collected to obtain the database in this paper, which includes a total of 158 test results, as shown in Table 1. Since the number of samples is too large, a matrix analysis plot is drawn to show the data (Figure 5), which examines the correlation between the input and output variables. It is indicated that there is a negative correlation between the porosity and the remaining four input variables. (The Corr in Figure 5 means Pearson correlation coefficient). Moreover, longitudinal wave velocity, Schmidt hammer rebound number, point load strength, and Young’s modulus are positively correlated with each other. To evaluate whether there are outliers in the data, a violin plot is drawn, as shown in Figure 6. The data we utilized in this study is evenly distributed. There are no obvious abnormal data in this database.

RESULT ANALYSIS

Parameters Initialization

Setting a proper ratio between the training samples and test samples in the dataset is significant. According to the Pareto principle, the training group number and the test group number should account for about 80% and 20% of the total samples (Forman and Peniwati, 1998; Yu et al., 2021). On the basis of this rule, in this study, the training group was set at 128 groups, accounting for 81%, and the test group was set at 30 groups, accounting for 19%. The initial parameters of the proposed six hybrid optimization models—SOA-BP, GWO-BP, WOA-BP, BSA-BP, LSO-BP and FA-BP are shown in Table 2.

Predicted Results

After using the eight models to predict the UCS values, the actual values and the predicted values are shown in Figure 7. It is found that there are some big errors in the BP and RF models. The predicted values related to these six hybrid models are closer to the actual values.

Evaluation Method of Prediction Models

To evaluate the predicted results of the mentioned eight models, four parameters—RMSE, MAPE, R^2 , a10 index were introduced. RMSE is a machine learning metric that measures the difference between the predicted and real values. The prediction model’s prediction effect improves as the RMSE decreases. (Barnston, 1992). RMSE could be calculated as:

$$RMSE = \sqrt{\sum_{i=1}^{N_0} (\hat{y}_i - y_i)^2 / N_0} \quad (13)$$

Where N_0 is the sample number in the test set, \hat{y}_i is the predicted result and y_i is the actual value.

MAPE calculates the difference between the expected and actual value. MAPE has a range greater than or equal to 0. Once the MAPE is close to 0, it is indicated that the corresponding model has little errors. When MAPE is greater than 1, the model is called as inferior model (Bollen et al., 2011). MAPE could be calculated as follows:

$$MAPE = \frac{1}{N_0} \sum_{i=1}^{N_0} \left| \frac{\hat{y}_i - y_i}{y_i} \right| \times 100 \quad (14)$$

The coefficient of determination. When least squares are used for parameter estimation, R^2 is the ratio of explained sum of squares to sum of squares of deviations. And the larger the R^2 is, the more accurate the model is and the more significant the regression effect is. R^2 is a value between 0 and 1, where the closer it goes to 1, the better the model fits. It is generally considered that models with a R^2 over 0.8 are good. R^2 could be obtained as:

$$R^2 = 1 - \frac{\sum_{i=1}^{N_0} (y_i - \hat{y}_i)^2}{\sum_{i=1}^{N_0} (y_i - \bar{y})^2} \quad (15)$$

Where \bar{y} is the mean of predicted values.

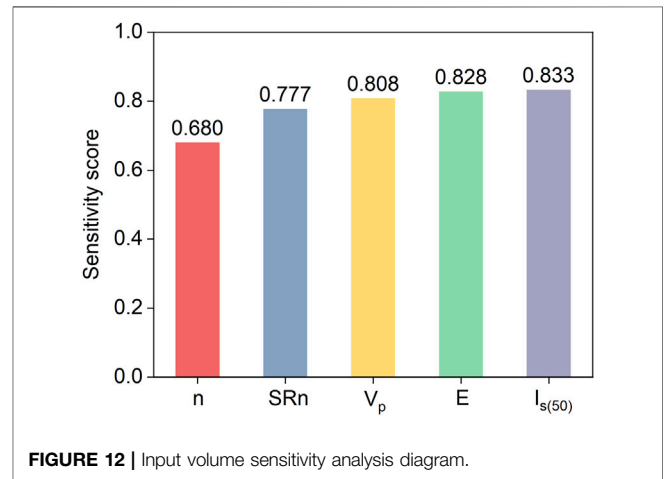
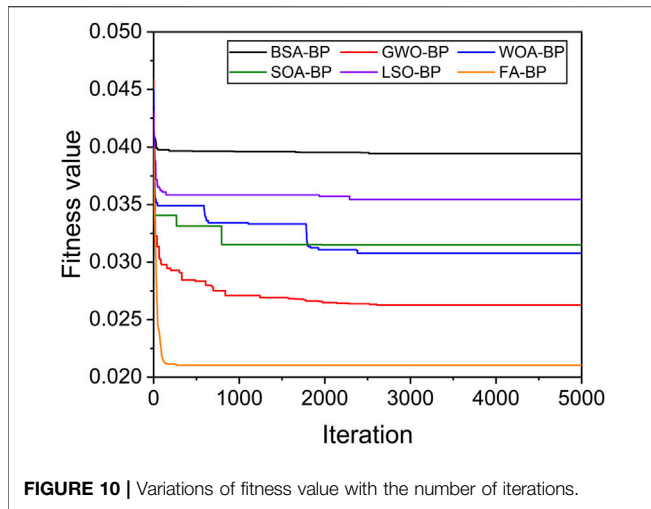
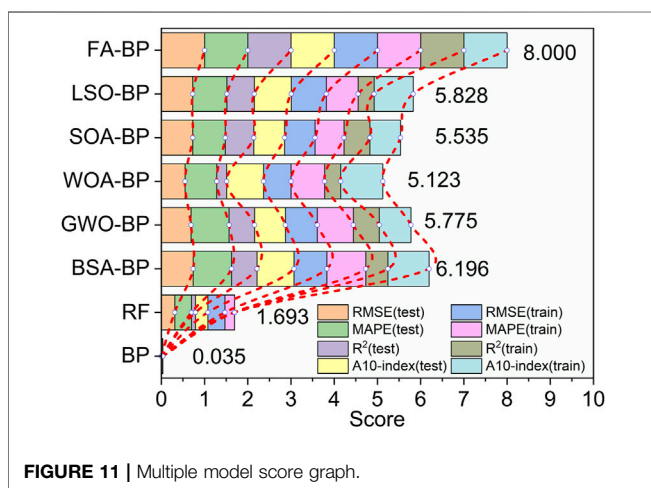


TABLE 3 | List of evaluation parameters.

Model		RMSE	Score	MAPE	Score	R ²	Score	A10-index	Score
Training	BP	12.859	0.000	0.190	0.000	0.941	0.029	0.608	0.006
	RF	9.846	0.349	0.163	0.223	0.940	0.000	0.606	0.000
	BSA-BP	7.058	0.672	0.081	0.901	0.958	0.514	0.928	0.953
	GWO-BP	7.035	0.675	0.079	0.917	0.961	0.600	0.827	0.654
	WOA-BP	8.009	0.562	0.096	0.777	0.953	0.371	0.936	0.976
	SOA-BP	6.789	0.703	0.109	0.669	0.965	0.714	0.889	0.837
	LSO-BP	6.622	0.723	0.101	0.736	0.953	0.371	0.912	0.905
	FA-BP	4.228	1.000	0.069	1.000	0.975	1.000	0.944	1.000
Testing	BP	12.058	0.000	0.210	0.000	0.941	0.000	0.733	0.000
	RF	9.832	0.310	0.153	0.388	0.945	0.091	0.800	0.286
	BSA-BP	6.776	0.736	0.079	0.891	0.967	0.591	0.933	0.855
	GWO-BP	7.136	0.686	0.080	0.884	0.967	0.591	0.900	0.714
	WOA-BP	8.130	0.547	0.102	0.735	0.951	0.227	0.933	0.855
	SOA-BP	6.854	0.725	0.099	0.755	0.970	0.659	0.900	0.714
	LSO-BP	6.854	0.725	0.094	0.789	0.969	0.636	0.933	0.855
	FA-BP	4.883	1.000	0.063	1.000	0.985	1.000	0.967	1.000



a10 index is a novel index in statistics. It is the ratio of the number of scatter points falling between $\hat{y}_i = 0.9y_i$ and $\hat{y}_i = 1.1y_i$ to the total number of samples in the test set. a10 lies between 0 and 1. If the a10 is close to 1, the corresponding model is better. a10 can be calculated by the following equation (Cevik et al., 2011):

$$a10 - index = \frac{m10}{M} \tag{16}$$

Where $m10$ is the number in test set falling between $\hat{y}_i = 0.9y_i$ and $\hat{y}_i = 1.1y_i$, M is the total number of samples in the test set.

Though the above four evaluate indexes, it is indicated that the FA-BP model is the best model in UCS prediction, with the RMSE of 4.883, a MAPE of 0.063, an R^2 of 0.985 and an a10 index of 0.967. The worst in the hybrid models was WOA-BP with the RMSE value of 8.130, the MAPE value of 0.102, the R^2 of 0.951, and the a10 index of 0.933. The other hybrid models all have an R^2 of 0.95

or higher, which shows that the hybrid models have better prediction results. On the contrary, the BP model had the RMSE value of 12.058, the MAPE value of 0.21, the R^2 of 0.941, and an a10 of 0.733. In the random forest, there are the RMSE value of 9.832, MAPE value of 0.153, R^2 of 0.945, and the a10 was 0.800. Their effects were all relatively poor. The relationship between the predicted and actual values was drawn in **Figure 8**. It could be seen in **Figure 8** that all points are distributed on both sides of the perfect fit line. The data points corresponding to the FA-BP model are closest to the perfect fit line, and the data points are the most discrete in the BP model.

To further evaluate the predict results of all prediction models, the Taylor diagrams were drawn to show the relevance of the standard deviation, root mean square error and correlation coefficient (Ciesielski et al., 2002), the relationship in these three parameters in Taylor diagrams could be obtained by:

$$R = \frac{\frac{1}{Z} \sum_1^Z (l_n - \bar{l})(m_n - \bar{m})}{\sigma_l \sigma_m} \quad (17)$$

Where R is the correlation coefficient, Z is the number of discrete points, l_n and m_n is discrete variables, σ_l and σ_m is the standard deviation of l and m , \bar{l} and \bar{m} are the means of σ_l and σ_m , respectively.

All Taylor diagrams are listed in **Figure 9**, and all the fitness value curves with the increasing iterations were collected, as shown in **Figure 10**. It could be seen from **Figure 9** that the point corresponding to the FA-BP model is closest to the observation point in the 2D coordinates, indicating that this model has minimal prediction error. On the contrary, the point corresponding to the BP model is the furthest from the observation point, indicating that the prediction effect is poor. Moreover, the fitness curve corresponding to the FA-BP model decreases faster than that of other prediction models.

COMPREHENSIVE EVALUATION OF UCS PREDICTION MODELS

To further analyze and compare the prediction performance and algorithm stability of these six hybrid models and two single models, we scored and evaluated the evaluation metrics for each model training set and testing set. Within the widely used grading method, all evaluation indexes need to be ordered, and then graded (Yin et al., 2021). However, two similar values may be classified into different levels in this method. To avoid this condition, we only calculate the scores for each model. The same evaluation index of each model is normalized by the following equation (Rao et al., 2008):

$$y_i = \frac{x_i - \min_0}{\max_0 - \min_0} \quad (18)$$

Where y_i is the normalized value, x_i is one of the evaluation indexes, \min_0 and \max_0 are the minimum and maximum values of each evaluation index, respectively.

After the normalization, all normalized values are in the range of 0–1. Noting that the larger R^2 value and a10 index value represent better models. On the contrary, if RMSE and MAPE are smaller, the

corresponding model is better. When calculating the evaluation score of these four evaluation indexes, the evaluation scores for RMSE and MAPE are the difference between 1 and their corresponding normalized values. For the R^2 value and a10 index value, the evaluation score is equal to their normalized values. By replacing the traditional simple grading method with this standardized evaluation index, the problem of excessive disparity between the scores of close evaluation parameters can be solved (Chen et al., 2013).

All the obtained evaluation scores according to the calculation procedures were listed in **Table 3** and **Figure 11**. As can be seen from **Table 3**, the scoring parameters of the training set and the testing set are relatively close in the same algorithm, which indicates that the algorithms are stable. Meanwhile, in order to better show the prediction effects of the eight algorithms, we accumulate the scores of the training and test sets of the algorithms to get the final scores of the algorithms, as shown in **Figure 11**. It is indicated from the evaluation results that the best prediction model is FA-BP, with a full score of 8. While the other five hybrid algorithms all scored between 5.123 and 6.196, the single model RF only scored 1.693 and the BP neural network scored 0.035. Noting that even if the other five hybrid models all have a worse effect than the FA-BP model, their predicted results are better than the unoptimized model–BP model and RF model.

SENSITIVITY ANALYSIS

It is evident from previous sections that the five input variables in this paper all have an obvious correlation with the UCS, but the significance level of each input variable is not yet known, and it needs to be further studied. Mutual information was often used by scholars in the information theory as a parameter to evaluate the correlation between two objects (Maes et al., 1997). Furthermore, normalized mutual information (NMI) can also be used to evaluate the relationships between each feature label. To make the overall predictive modeling scheme more convincing, the five input variables are evaluated by means of the Normalized Mutual Information (NMI) as a means of determining the importance of each variable parameter to the model. Mutual information I could be obtained as follows.

$$I(X;Y) = \sum_x \sum_y p(x,y) \log \frac{p(x,y)}{p(x)p(y)} \quad (19)$$

Where X and Y are two random variables, $p(x,y)$ is the joint distribution of these two random variables, and $p(x)$, $p(y)$ is the marginal distribution of x and y . Mutual information $I(X;Y)$ is the relative entropy of the joint distribution $p(x,y)$ and the product distributions $p(x)p(y)$. To compare the significance of all input variables, the mutual information should be normalized by the following equation:

$$NMI(X;Y) = \frac{2I(X;Y)}{H(X) + H(Y)} \quad (20)$$

Where $NMI(X;Y)$ is the normalized mutual information, and $H(X)$ and $H(Y)$ are the information entropy of the X and Y , respectively. On the basis of the values of the normalized

mutual information, the significance levels of these input variables using in UCS prediction can be obtained, as shown in **Figure 12**. The sensitivity scores of the four quantities—Schmidt hammer rebound number, rock longitudinal wave velocity, point load test strength, and Young's modulus are 0.777, 0.808, 0.828, and 0.833 respectively. Porosity has a low sensitivity score of 0.68. On the whole, the five parameters selected in this paper are in line with the requirements.

CONCLUSION

In this paper, to predict the UCS of rock samples with the collected database with the artificial intelligence algorithm, six hybrid models—BSA-BP, GWO-BP, WOA-BP, SOA-BP, LSO-BP, FA-BP, and two classic models—BP and RF were developed. The predicted results obtained from the developed eight models were compared through four evaluation indexes and comprehensive scores. The following conclusions could be drawn:

- (1) When predicting the UCS, six hybrid models based on the swarm intelligence optimization algorithms in this study are all significantly more accurate and significantly better than the BP neural network model and random forest model.
- (2) The prediction accuracy of the used eight models from high to low is the FA-BP model, BSA-BP model, GWO-BP model, LSO-BP model, SOA-BP model, WOA-BP model, RF model, BP model. Among them, the FA-BP hybrid model showed the best comprehensive performance in six hybrid models and two single models. When carrying out

REFERENCES

- Aljarah, I., Faris, H., and Mirjalili, S. (2016). Optimizing Connection Weights in Neural Networks Using the Whale Optimization Algorithm. *Soft Comput.* 22 (1), 1–15. doi:10.1007/s10462-019-09704-910.1007/s00500-016-2442-1
- Armaghani, D. J., Tonnizam Mohamad, E., Momeni, E., Monjezi, M., and Sundaram Narayanasamy, M. (2015). Prediction of the Strength and Elasticity Modulus of Granite through an Expert Artificial Neural Network. *Arab. J. Geosci.* 9 (1), 48. doi:10.1007/s12517-015-2057-3
- Barnston, A. G. (1992). Correspondence Among the Correlation, RMSE, and Heidke Forecast Verification Measures; Refinement of the Heidke Score. *Wea. Forecast.* 7 (4), 6992–7709. doi:10.1175/1520-0434(1992)007<0699:catcra>2.0.co;2
- Barton, N. R., Løset, F., Lien, R., and Lunde, J. (1980). Application of the Q-System in Design Decisions Concerning Dimensions and Appropriate Support for Underground Installations. In: *Editor M. Bergman, Subsurface space, New York: Pergamon*, 2, 553–561. doi:10.1016/B978-1-4832-8421-7.50080-6
- Barton, N. (2002). Some New Q-Value Correlations to Assist in Site Characterisation and Tunnel Design. *Int. J. Rock Mech. Min. Sci.* 39 (2), 185–216. doi:10.1016/s1365-1609(02)00011-4
- Bieniawski, Z. T. (1978). Determining Rock Mass Deformability: Experience from Case Histories. *Int. J. Rock Mech. Min. Sci. Geomechanics Abstr.* 15 (5), 237–247. doi:10.1016/0148-9062(78)90956-7
- Bollen, J., Mao, H., and Zeng, X. (2011). Twitter Mood Predicts the Stock Market. *J. Comput. Sci.* 2 (1), 1–8. doi:10.1016/j.jocs.2010.12.007
- Breiman, L. (2001). Random Forests. *Mach. Learn.* 45, 5–32. doi:10.1023/a:1010933404324
- Broch, E., and Franklin, J. A. (1972). The Point-Load Strength Test. *Int. J. Rock Mech. Min. Sci. Geomechanics Abstr.* 9 (6), 669–676. doi:10.1016/0148-9062(72)90030-7
- Bureau, A., Dupuis, J. e., Falls, K., Lunetta, K. L., Hayward, B., Keith, T. P., et al. (2005). Identifying SNPs Predictive of Phenotype Using Random Forests. *Genet. Epidemiol.* 28 (2), 171–182. doi:10.1002/gepi.20041
- Cevik, A., Sezer, E. A., Cabalar, A. F., and Gokceoglu, C. (2011). Modeling of the Uniaxial Compressive Strength of Some Clay-Bearing Rocks Using Neural Network. *Appl. Soft Comput.* 11 (2), 2587–2594. doi:10.1016/j.asoc.2010.10.008
- Chen, W., Yan, E. C., Cui, X. J., and Zhang, D. (2018). Variable Weight Interval Fuzzy Evaluation Method for Rock Mass Quality. *Yangtze River.* 49 (18), 72–74. doi:10.16232/j.cnki.1001-4179.2018.18.014
- Ciesielski, M. J., Kalla, P., Zheng, Z., and Rouzeyre, B. (2002). “Taylor Expansion Diagrams: A Compact, Canonical Representation with Applications to Symbolic Verification,” in *Proceedings 2002 Design, Automation and Test in Europe Conference and Exhibition, Paris, France, 04-08 March 2002 (IEEE)*. doi:10.1109/DATE.2002.998286
- Dehghan, S., Sattari, G., Chehreh Chelgani, S., and Aliabadi, M. (2010). Prediction of Uniaxial Compressive Strength and Modulus of Elasticity for Travertine Samples Using Regression and Artificial Neural Networks. *Min. Sci. Technol. (China)* 20 (1), 41–46. doi:10.1016/s1674-5264(09)60158-7
- Dhiman, G., and Kumar, V. (2019). Seagull Optimization Algorithm: Theory and its Applications for Large-Scale Industrial Engineering Problems. *Knowledge-Based Syst.* 165, 169–196. doi:10.1016/j.knsys.2018.11.024
- Dhiman, G., Singh, K. K., Slowik, A., Chang, V., Yildiz, A. R., Kaur, A., et al. (2020). EMoSOA: a New Evolutionary Multi-Objective Seagull Optimization

the UCS prediction, the FA-BP model should be considered first.

- (3) In the sensitivity analysis, porosity, Schmidt hammer rebound number, longitudinal wave velocity, point load strength, and Young's modulus have the higher scores of 0.680, 0.777, 0.808, 0.828, and 0.833, respectively. They all could be utilized as input quantities when conducting the UCS prediction.

DATA AVAILABILITY STATEMENT

The original contributions presented in the study are included in the article/Supplementary Material, further inquiries can be directed to the corresponding author.

AUTHOR CONTRIBUTIONS

Investigation, YL and SZ; methodology, YL and SZ; writing-original draft preparation, YL and SZ; writing-review and editing, NJ and XL; supervision, XL; data curation, YL and SN; visualization, SN; funding acquisition, XL and NJ. All authors have read and agreed to the published version of the manuscript.

FUNDING

This project was supported by the National Natural Science Foundation of China (42072309, 41807265) and the Hubei Key Laboratory of Blasting Engineering Foundation (HKLBEF202002).

- Algorithm for Global Optimization. *Int. J. Mach. Learn. Cyber.* 12 (2), 571–596. doi:10.1007/s13042-020-01189-1
- Dinçer, İ., Acar, A., and Ural, S. (2008). Estimation of Strength and Deformation Properties of Quaternary Caliche Deposits. *Bull. Eng. Geol. Environ.* 67 (3), 353–366. doi:10.1007/s10064-008-0146-1
- Emary, E., Zawbaa, H. M., and Hassanien, A. E. (2016). Binary Grey Wolf Optimization Approaches for Feature Selection. *Neurocomputing* 172, 371–381. doi:10.1016/j.neucom.2015.06.083
- Fister, I., Fister, I., Yang, X., and Brest, J. (2013). A Comprehensive Review of Firefly Algorithms. *Swarm Evol. Comput.* 13, 34–36. doi:10.1016/j.swevo.2013.06.001
- Forman, E., and Peniwati, K. (1998). Aggregating Individual Judgments and Priorities with the Analytic Hierarchy Process. *Eur. J. Operational Res.* 108 (1), 165–169. doi:10.1016/s0377-2217(97)00244-0
- Gandomi, A. H., Yang, X.-S., and Alavi, A. H. (2011). Mixed Variable Structural Optimization Using Firefly Algorithm. *Comput. Struct.* 89 (23–24), 2325–2336. doi:10.1016/j.compstruc.2011.08.002
- Gandomi, A. H., Yang, X.-S., Talatahari, S., and Alavi, A. H. (2013). Firefly Algorithm with Chaos. *Commun. Nonlinear Sci. Numer. Simul.* 18 (1), 89–98. doi:10.1016/j.cnsns.2012.06.009
- Hao, X., Du, W., Jiang, Y., Tannant, D., Zhao, Y., and Guo, Y. (2018). Influence of Bedding and Cleats on the Mechanical Properties of a Hard Coal. *Arab. J. Geosci.* 11 (9), 1–17. doi:10.1007/s12517-018-3541-3
- Hoek, E., and Brown, E. (1997). Practical Estimates of Rock Mass Strength. *Int. J. Rock Mech. Mining Sci.* 34 (8), 1165–1186. doi:10.1016/s1365-1609(97)80069-x
- He, M., Zhang, Z., Ren, J., Huan, J., Li, G., Chen, Y., et al. (2019). Deep Convolutional Neural Network for Fast Determination of the Rock Strength Parameters Using Drilling Data. *Int. J. Rock Mech. Min. Sci.* 123, 104084. doi:10.1016/j.ijrmms.2019.104084
- Kayabasi, A., Gokceoglu, C., and Ercanoglu, M. (2003). Estimating the Deformation Modulus of Rock Masses: a Comparative Study. *Int. J. Rock Mech. Min. Sci.* 40 (1), 55–63. doi:10.1016/s1365-1609(02)00112-0
- Lashkaripour, G. R. (2002). Predicting Mechanical Properties of Mudrock from Index Parameters. *Bull. Eng. Geol. Environ.* 61 (1), 73–77. doi:10.1007/s100640100116
- Leite, M., and Ferland, F. (2001). Determination of Unconfined Compressive Strength and Young's Modulus of Porous Materials by Indentation Tests. *Eng. Geol.* 59 (3–4), 267–280. doi:10.1016/s0013-7952(00)00081-8
- Liu, Z., Yan, D., and Niu, X. (2020). Insights into Pore Structure and Fractal Characteristics of the Lower Cambrian Niutitang Formation Shale on the Yangtze Platform, South China. *J. Earth Sci.* 31 (1), 169–180. doi:10.1007/s12583-020-1259-0
- Maes, F., Collignon, A., Vandermeulen, D., Marchal, G., and Suetens, P. (1997). Multimodality Image Registration by Maximization of Mutual Information. *IEEE Trans. Med. Imaging* 16 (2), 187–198. doi:10.1109/42.563664
- Mafarja, M. M., and Mirjalili, S. (2017). Hybrid Whale Optimization Algorithm with Simulated Annealing for Feature Selection. *Neurocomputing* 260, 302–312. doi:10.1016/j.neucom.2017.04.053
- Mahmoodzadeh, A., Mohammadi, M., Hashim Ibrahim, H., Nariman Abdulhamid, S., Ghafoor Salim, S., Farid Hama Ali, H., et al. (2021). Artificial Intelligence Forecasting Models of Uniaxial Compressive Strength. *Transp. Geotech.* 27, 100499. doi:10.1016/j.trgeo.2020.100499
- Majdi, A., and Beiki, M. (2010). Evolving Neural Network Using a Genetic Algorithm for Predicting the Deformation Modulus of Rock Masses. *Int. J. Rock Mech. Min. Sci.* 47 (2), 246–253. doi:10.1016/j.ijrmms.2009.09.011
- Meng, X.-B. X., Gao, X. Z., Lu, L., Liu, Y., and Zhang, H. (2015). A New Bio-Inspired Optimisation Algorithm: Bird Swarm Algorithm. *J. Exp. Theor. Artif. Intell.* 28 (4), 673–687. doi:10.1080/0952813x.2015.1042530
- Meng, X., Yu, L., Gao, X., and Zhang, H. (2015). “A New Bio-Inspired Algorithm: Chicken Swarm Optimization,” in International Conference in Swarm Intelligence (Advances in Swarm Intelligence), 8794, 89–94. doi:10.1007/978-3-319-11857-4_10
- Meulenkamp, F., and Grima, M. A. (1999). Application of Neural Networks for the Prediction of the Unconfined Compressive Strength (UCS) from Equotip Hardness. *Int. J. Rock Mech. Min. Sci.* 36 (1), 29–39. doi:10.1016/s0148-9062(98)00173-9
- Miramontes, I., Guzman, J., Melin, P., and Prado-Arechiga, G. (2018). Optimal Design of Interval Type-2 Fuzzy Heart Rate Level Classification Systems Using the Bird Swarm Algorithm. *Algorithms* 11 (12), 206. doi:10.3390/a11120206
- Mirjalili, S., and Lewis, A. (2016). The Whale Optimization Algorithm. *Adv. Eng. Softw.* 95, 51–67. doi:10.1016/j.advengsoft.2016.01.008
- Mirjalili, S., Mirjalili, S. M., and Lewis, A. (2014). Grey Wolf Optimizer. *Adv. Eng. Softw.* 69, 46–61. doi:10.1016/j.advengsoft.2013.12.007
- Mishra, D. A., and Basu, A. (2013). Estimation of Uniaxial Compressive Strength of Rock Materials by Index Tests Using Regression Analysis and Fuzzy Inference System. *Eng. Geol.* 160, 54–68. doi:10.1016/j.enggeo.2013.04.004
- Mitri, H. S., Edrissi, R., and Henning, J. G. (1994). *Finite Element Modelling of Cable-Bolted Stopes in Hard Rock Underground Mines*. Presented at the SME Annual Meeting, New Mexico, Albuquerque, 94–116.
- Mohamad, E. T., Jahed Armaghani, D., Momeni, E., and Alavi Nezhad Khalil Abad, S. V. (2015). Prediction of the Unconfined Compressive Strength of Soft Rocks: a PSO-Based ANN Approach. *Bull. Eng. Geol. Environ.* 74 (3), 745–757. doi:10.1007/s10064-014-0638-0
- Momeni, E., Jahed Armaghani, D., Hajihassani, M., and Mohd Amin, M. F. (2015). Prediction of Uniaxial Compressive Strength of Rock Samples Using Hybrid Particle Swarm Optimization-Based Artificial Neural Networks. *Measurement* 60, 50–63. doi:10.1016/j.measurement.2014.09.075
- Nicholson, G. A., and Bieniawski, Z. T. (1990). A Nonlinear Deformation Modulus Based on Rock Mass Classification. *Int. J. Min. Geol. Eng.* 8 (3), 181–202. doi:10.1007/bf01554041
- Panagant, N., Pholdee, N., Bureerat, S., Kaen, K., Yıldız, A. R., and Sait, S. M. (2020). Seagull Optimization Algorithm for Solving Real-World Design Optimization Problems. *Mater. Test.* 62 (6), 640–644. doi:10.3139/120.111529
- Rao, Y., Lee, Y., Jarjoura, D., Ruppert, A., Liu, C., and Hsu, J. (2008). A Comparison of Normalization Techniques for MicroRNA Microarray Data. *Stat. Appl. Genet. Mol. Biol.* 7 (1). doi:10.2202/1544-6115.1287
- Rezaei, M., Majidi, A., and Monjezi, M. (2012). An Intelligent Approach to Predict Unconfined Compressive Strength of Rock Surrounding Access Tunnels in Longwall Coal Mining. *Neural Comput. Applic* 24 (1), 233–241. doi:10.1007/s00521-012-1221-x
- Sachpazis, C. I. (1990). Correlating Schmidt Hardness with Compressive Strength and Young's Modulus of Carbonate Rocks. *Bull. Int. Assoc. Eng. Geol.* 42 (1), 75–83. doi:10.1007/bf02592622
- Shan, P. F., and Lai, X. P. (2018). Numerical Simulation of the Fluid-Solid Coupling Process during the Failure of a Fractured Coal-Rock Mass Based on the Regional Geostress. *Transp. Porous Med.* 124 (3), 1061–1079. doi:10.1007/s11242-018-1110-6
- Kishor, A., and Singh, P.K. (2016). Empirical Study of Grey Wolf Optimizer. *In Proc. Fifth Int. Conf. Soft Computing for Problem Solving* 436, 1037–49. doi:10.1007/978-981-10-0448-3-87
- Stroffek, E., and Lesso, I. (2001). Acoustic Method for Measurement of Young's Modulus of Steel Wire Ropes. *Metalurgija* 40 (4), 219–221.
- Tsiambaos, G., and Sabatakakis, N. (2004). Considerations on Strength of Intact Sedimentary Rocks. *Eng. Geol.* 72 (3–4), 261–273. doi:10.1016/j.enggeo.2003.10.001
- Tuğrul, A., and Zarif, I. (1999). Correlation of Mineralogical and Textural Characteristics with Engineering Properties of Selected Granitic Rocks from Turkey. *Eng. Geol.* 51 (4), 303–317. doi:10.1016/s0013-7952(98)00071-410.1016/s0013-7952(98)00071-4
- Ulusay, R., and Gokceglu, C. (1998). An Experimental Study on the Size Effect in Block Punch Index Test and its General Usefulness. *Int. J. Rock Mech. Min. Sci.* 35 (4–5), 628–629. doi:10.1016/s0148-9062(98)00024-2
- Varol Altay, E., and Alatas, B. (2019). Bird Swarm Algorithms with Chaotic Mapping. *Artif. Intell. Rev.* 53 (2), 1373–1414. doi:10.1007/s10462-019-09704-9
- Xue, X., and Wei, Y. (2020). A Hybrid Modelling Approach for Prediction of UCS of Rock Materials. *Comptes Rendus. Mécanique* 348 (3), 235–243. doi:10.5802/crmeca.17
- Yagiz, S. (2011). Correlation between Slake Durability and Rock Properties for Some Carbonate Rocks. *Bull. Eng. Geol. Environ.* 70 (3), 377–383. doi:10.1007/s10064-010-0317-8
- Yan, Z., and Zeng, L. (2013). “The BP Neural Network with MATLAB,” in 2013 International Conference on Electrical, Control and Automation Engineering (ECAE 2013), December 1–2, 2013 (Hong Kong: ECAE).
- Yaşar, E., and Erdoğan, Y. (2004). Estimation of Rock Physicomechanical Properties Using Hardness Methods. *Eng. Geol.* 71 (3–4), 281–288. doi:10.1016/s0013-7952(03)00141-8

- Yazdani, M., and Jolai, F. (2016). Lion Optimization Algorithm (LOA): A Nature-Inspired Metaheuristic Algorithm. *J. Comput. Des. Eng.* 3 (1), 24–36. doi:10.1016/j.jcde.2015.06.003
- Yilmaz, I., and Sendir, H. (2002). Correlation of Schmidt Hardness with Unconfined Compressive Strength and Young's Modulus in Gypsum from Sivas (Turkey). *Eng. Geol.* 66 (3–4), 211–219. doi:10.1016/s0013-7952(02)00041-8
- Yin, X., Liu, Q., Huang, X., and Pan, Y. (2022). Perception Model of Surrounding Rock Geological Conditions Based on TBM Operational Big Data and Combined Unsupervised-Supervised Learning. *Tunn. Undergr. Space Technol.* 120, 104285. doi:10.1016/j.tust.2021.104285
- Yin, X., Liu, Q., Pan, Y., Huang, X., Wu, J., and Wang, X. (2021). Strength of Stacking Technique of Ensemble Learning in Rockburst Prediction with Imbalanced Data: Comparison of Eight Single and Ensemble Models. *Nat. Resour. Res.* 30 (2), 1795–1815. doi:10.1007/s11053-020-09787-0
- Yu, Z., Shi, X., Miao, X., Zhou, J., Khandelwal, M., Chen, X., et al. (2021). Intelligent Modeling of Blast-Induced Rock Movement Prediction Using Dimensional Analysis and Optimized Artificial Neural Network Technique. *Int. J. Rock Mech. Min. Sci.* 143, 104794. doi:10.1016/j.ijrmms.2021.104794
- Yu, Z., Shi, X., Qiu, X., Zhou, J., Chen, X., and Gou, Y. (2020b). Optimization of Postblast Ore Boundary Determination Using a Novel Sine Cosine Algorithm-Based Random Forest Technique and Monte Carlo Simulation. *Eng. Optim.* 53 (9), 1467–1482. doi:10.1080/0305215x.2020.1801668
- Yu, Z., Shi, X., Zhou, J., Chen, X., Miao, X., Teng, B., et al. (2019). Prediction of Blast-Induced Rock Movement during Bench Blasting: Use of Gray Wolf Optimizer and Support Vector Regression. *Nat. Resour. Res.* 29 (2), 843–865. doi:10.1007/s11053-019-09593-3
- Yu, Z., Shi, X., Zhou, J., Chen, X., and Qiu, X. (2020a). Effective Assessment of Blast-Induced Ground Vibration Using an Optimized Random Forest Model Based on a Harris Hawks Optimization Algorithm. *Appl. Sci.* 10 (4), 1403. doi:10.3390/app10041403
- Yu, Z., Shi, X., Zhou, J., Gou, Y., Huo, X., Zhang, J., et al. (2020c). A New Multikernel Relevance Vector Machine Based on the HPSOGWO Algorithm for Predicting and Controlling Blast-Induced Ground Vibration. *Eng. Comput.* 38 (2), 1905–1920. doi:10.1007/s00366-020-01136-2

Conflict of Interest: The authors declare that the research was conducted in the absence of any commercial or financial relationships that could be construed as a potential conflict of interest.

Publisher's Note: All claims expressed in this article are solely those of the authors and do not necessarily represent those of their affiliated organizations, or those of the publisher, the editors and the reviewers. Any product that may be evaluated in this article, or claim that may be made by its manufacturer, is not guaranteed or endorsed by the publisher.

Copyright © 2022 Lei, Zhou, Luo, Niu and Jiang. This is an open-access article distributed under the terms of the Creative Commons Attribution License (CC BY). The use, distribution or reproduction in other forums is permitted, provided the original author(s) and the copyright owner(s) are credited and that the original publication in this journal is cited, in accordance with accepted academic practice. No use, distribution or reproduction is permitted which does not comply with these terms.